JJBS

Volume 16, Number 1,March 2023
ISSN 1995-6673
Pages 41 – 53
https://doi.org/10.54319/jjbs/160107

Jordan Journal of Biological Sciences

Astragalus sarcocolla Gum-mediated a Novel Green-synthesis of Biologically Active Silver-Nanoparticles with Effective Anticancer and Antimicrobial activities

Abeer A. Abd El Aty[1,*], Shifaa O. Alshammari[1], Reem M. Alharbi[1], Ahmed AF. Soliman[2]

[1]*Department of Biology, College of Science, University of Hafr Al Batin, P.O. Box 1803, Hafr Al Batin, Saudi Arabia;* [2] *Drug Bioassay-Cell Culture Laboratory, Pharmacognosy Department, National Research Center, Dokki, Giza, 12622, Egypt.*

Received: May 4, 2022; Revised: June 28, 2022; Accepted: July 6, 2022

Abstract

Cancer diseases and microbial infections are the subject of several ongoing recent researches. In this paper, aqueous extract of red and yellow *Astragalus sarcocolla* gum was used as safe and green agent, for the synthesis of novel biologically active silver-nanoparticles. Six silver nanoparticles (AgNPs) with different characters were obtained using *sarcocolla* gum at (5, 10 and 20 mg/ml (w/v)) concentrations. All biosynthesized AgNPs were characterized using UV–visible spectroscopy, Transmission Electron Microscopy (TEM), and Dynamic light scattering (DLS). Cytotoxic effect of *sarcocolla* gum-AgNPs against five human cancer cells and one normal cells was determined using the MTT (3-(4, 5-dimethylthiazol-2-yl)-2, 5-diphenyltetrazolium bromide) assay. The semi rounded particles formed from 5mg/ml red gum (AgNPs-RG1) and having 9.23±3.66 nm size range were the most active and possessed high cytotoxic effect against, A549 lung, pc3 prostate, Mcf-7 breast and paca2 pancreatic cancers, with IC_{50} values (88.4,75.6, 72.2& 55.0 ug/ml, respectively), but showed low cytotoxic effect (20 % at 100ug/ml) against human normal cells (BJ-1). On the other hand, the spherical to cubic shaped nanoparticles obtained from 5mg/ml yellow gum (AgNPs-YG1) with 10.92 ± 5.48 nm size range, showed good cytotoxic effect against three cancer cells (PC3 prostate, MCF-7 breast and paca2 pancreatic) with IC_{50} values (75.0, 82.8 and 81,6ug/ml respectively), and normal cells(BJ-1) with IC_{50} value (81.8ug/ml). Antibacterial and antifungal activities of the synthesized red and yellow gum-mediated AgNPs with different sizes and shapes were also investigated. Particles biosynthesized from 5 and 10 mg/ml red gum (AgNPs-RG1, RG2) and 5mg/ml yellow gum (AgNPs-YG1) exhibited broad spectrum antimicrobial effects against all tested pathogenic gram-positive, gram-negative bacterial strains, unicellular yeast and filamentous fungi. Based on these results, it can be concluded that the synthesized silver nanoparticles from low concentrations of *sarcocolla* gum have significant biomedical applications.

Keywords: Green-synthesis, *Astragalus sarcocolla* gum, Biosynthesis, AgNPs, Anticancer, Antimicrobial.

1. Introduction

Different microbial infection diseases and severe cancers are the most widely spread and diagnosed diseases worldwide (Mackey *et al*., 2014). Repeated use of current conventional treatments of synthetic antibiotics against microbial infection diseases, causes the antibiotic resistance, and inadequate treatments of these drugs (Bisht *et al*., 2010). On the other hand, using synthetic radiation therapy, surgery, generic drugs, chemotherapy, and hormone therapy did not show an effective result in cancer disease treatments (Qi *et. al.*, 2015; Akram *et al*., 2017). Therefore, more effort has been made to search for new low-cost materials with high efficiency for treating these diseases. The production of metal nano-particles made with natural biomolecules was considered as novel and effective alternative antimicrobial and anticancer modalities (Vasan *et al*., 2019).

Silver nanoparticles (AgNPs) are considered one of the most potential researched metal nanoparticles with high biological activities due to their unique physical properties, particularly their small size, large surface area, stability, and tunable size (Raghavendra *et al*., 2016; Pandey *et al*., 2016, Alharbi *et al.*, 2023). The biological applications of AgNPs have been greatly demonstrated in the fields of biotechnology, pharmaceuticals and medicine (Raghavendra *et al*., 2016; Lee and Jun, 2019). In addition, several researches indicated that involving the integration of nano-particles with biological molecules led to the development of antimicrobial agents, therapies in cancer, therapeutic medicines, drug delivery systems, labeling agents, etc. (Roy *et al*., 2015a, Song and Kim 2009, Kokila *et al.*, 2015, Daniel and Astruc 2004).

AgNPs are generally synthesized using various synthetic methods such as photochemical, chemical, electrochemical and γ-irradiation (Li *et al*., 2007; Raju *et al*., 2014). Most of these synthetic methods are hazardous due to application of toxic chemical agents which pose

* Corresponding author. e-mail: abeerab@uhb.edu.sa, aabass44@yahoo.com.

environmental problems and biological hazards (Mehndiratta *et al*., 2013). In recent times, much effort is being focused, by researchers, to prepare AgNPs using "green chemistry approaches", in which silver salts are biologically reduced to AgNPs using nontoxic and natural low cost polymers such as bacterial biomass (Abd El Aty and Zohair, 2020), Fungi (Abd El Aty *et al.*, 2020), algae (Alharbi *et al*., 2020), Yeasts (Ammar *et al.*, 2021), plant extracts (Parveen *et al*., 2016) and extracts of different natural gums, i.e., *kondagogu*-gum (Rastogi et al., 2014), *salmalia malabarica* gum (Murali krishna *et al.*, 2015) guar gum (Pandey and Mishra 2014, Pandey and Mishra, 2016), ghatti gum (Kora *et al.*, 2012). These biopolymers are used as both stabilizing and reducing agents (Demchenko *et al.*, 2020; Wang *et al.*, 2021). *Astragalus sarcocolla* a historical shrub, belongs to the Fabaceae family able to form the gum as a secondary metabolite. *Sarcocolla* gum is one of the most famous gum resins in Kingdom of Saudi Arabia used in folk medicine for treating wounds, flatulence and used as antiviral agent to prevent various winter diseases in children (Ababutain, 2017).

Based on the research articles published on the medicinal applications of the genus "*Astragalus*", we have noticed that *sarcocolla* gum resin has not been studied as a reducing and capping agent for biological synthesis of AgNPs. Therefore, the objective of this study is to explore the potential green synthesis of AgNPs with *Astragalus sarcocolla* gum aqueous extract as a reducing, capping, and stabilizing agent and ascertain characterization of gum-AgNPs. Also, the biological activity of silver-nanoparticles as antibacterial and anticancer agents was evaluated on Gram-positive and Gram-negative bacteria, yeast, fungi and five carcinoma cell lines for their potential biomedical applications.

2. Materials and Methods

2.1. Preparation of Astragalus sarcocolla gum aqueous extract

Sarcocolla red and yellow gum of the *Astragalus sarcocolla* tree was obtained from local herbarium market in Hafr Al Batin City, Saudi Arabia. Red (**RG**) and yellow (**YG**) gum was ground separately using ceramic mortar into a fine powder in a 100 ml Erlenmeyer flask. 1 g of fine powder along with 20 ml of distilled water was stirred for 60 min on magnetic starrier (60rpm and 30°C). Further, the aqueous extracts were centrifuged at 5000 cycle/min for 10 min., and the stock extracts of (50 mg/ml) concentration were stored at 4 °C for future studies.

2.2. Protein content

According to Lowry *et al.* (1951), the protein concentration in stock extracts of red and yellow gum was assayed.

2.3. Green-synthesis of silver nanoparticles

Three different concentrations of (5, 10, 20 mg/ml) were prepared from red and yellow stock aqueous extracts and evaluated for biosynthesis of nano-silver. 10 ml of each prepared concentration was mixed with 5 ml of 4mM $AgNO_3$ separately at 10 pH and incubated in a dark rotating shaker of 150 rpm and 28-30 °C for 24 hours (Abd El Aty *et al.*, 2020).

2.4. Characterization techniques

2.4.1. UV–visible spectroscopy

The formation of silver nanoparticles was initially detected by visual observation of color change from pale red and pale yellow to reddish-brown color. The bio-reduction of silver ions was monitored by UV–Visible spectrophotometer. The absorption spectrum of the aqueous filtrate was scanned in the range of 200–800 nm. The sharp peak given by UV visible spectrum indicated the formation of AgNPs at the absorption range 400–450 nm.

2.4.2. Transmission Electron Microscopy (TEM)

TEM analysis was performed to determine the morphology, size and shape of the silver nanoparticles. TEM measurements were done by (TEM; JEOL, JEM-2100, Japan) according to Ammar *et al*. (2021).

2.4.3. 2.4.3. Dynamic light scattering (DLS)

Zeta potential and distribution of particle size were measured using Dynamic Light Scattering (Particle Sizing Systems, Inc. Santa Barbara, California, USA) in the range of 0.1–1000 μm. Dynamic light scattering system (DLS) was used for the analysis of average size and distribution of particles in solution which gives the hydrodynamic diameter of particles.

2.5. Cytotoxicity assay

2.5.1. Cell culture

Cytotoxic assays were performed using five human cancer cell lines namely (A549 lung cancer, HCT116 colon cancer, MCF-7 breast cancer, PC3 prostate cancer, and paca2 pancreatic cancer) and one humane normal cell line (BJ-1), all cells purchased from the karolinska center, Department of oncology and pathology, Karolinska institute and hospital, Stockholm. Cancer cells were maintained in DMEM medium and DMEM F12 in case of normal cells. All media were supplemented with 10% fetal bovine serum and 100 μg ml^{-1} streptomycin, and 100 IU ml^{-1} penicillin. And then the cells were incubated at 37C^{o} in 5 %CO_2 and 95% humidity. Cells were sub-cultured using trypsin 0.15 % (Abd El Aty *et al.*, 2020; Alharbi *et al.*, 2020).

2.5.2. MTT Assay for testing cell viability

Cancer cells were seeded at a density of 1×10^4 and 1×10^5 (in case of normal cells) per well into 96-well plates in appropriate culture medium and pre-incubated for 24 h at 37°C humidified atmosphere containing 5% CO2. After that, the cells were treated for 48 h with different concentrations of sample (12.5, 25, 50 and 100 μg ml^{-1}) in the respective cell culture medium. Doxorubicin was used as positive control and 0.5 % DMSO was used as negative control. Cell viability was determined using the MTT (3-(4, 5-dimethylthiazol-2-yl)-2, 5-diphenyltetrazolium bromide) assay as described by Mosmann (1983). The equation used for calculation of percentage cytotoxicity was:

Percentage of cytotoxicity %= (1- (av(x) / (av(NC))) * 100

Where Av: average, X: absorbance of sample well measured at 595 nm with reference 690 nm, NC: absorbance of negative control measured at 595 nm with reference 690.

The IC_{50} values were determined using probit analysis and utilizing the SPSS computer program (SPSS for windows, statistical analysis software package / version 9 / 1989 SPSS Inc., Chicago, USA).

2.5.3. Cellular morphology

Microscopic examination of human tested cancer cell lines was checked by using Inverted microscope (Nikon, TMS-F, New York, USA).

2.6. Assessment of antimicrobial activity (Bioassay)

Silver-nanoparticles biosynthesized from aqueous extract of red gum (R1, R2, R3) and those prepared using aqueous extract of yellow gum (Y1, Y2, Y3) were tested against harmful pathogenic bacteria, yeast and fungi by the agar diffusion technique (Abd El Aty and Ammar, 2016).

2.6.1. Antibacterial assay

All prepared AgNPs were screened against pathogenic strains of Gram-positive (*Staphylococcus aureus* ATCC29213, *Bacillus subtilis* ATCC6633, *Lactobacillus cereus* ATCC14579) and Gram- negative (*Escherichia coli* ATCC25922, *Salmonella enterica* ATCC25566). Suspensions of all pathogenic strains were prepared and adjusted to be approximately (1×10^6 spores^{-ml}). 1 ml of each bacterial suspension was inoculated into a plate containing 50 ml of sterile nutrient agar medium (NA). Wells of about 15 mm in diameter were made in the solidified agar media and filled with 400 µl of AgNps colloidal solution, then they were left for 120 min at 4 ºC for compound diffusion. The plates were incubated for 24 h at 30 ºC for bacteria growth. The inhibition zones of all tested organisms were recorded in millimeters at three different points, and the average values are reported as Mean ± SD using MS Excel (Abd El Aty and Zohair, 2020).

2.6.2. Antifungal assay

The antifungal effects of biosynthesized AgNPs were tested against the unicellular yeast (*Candida albicans* ATCC10321) and filamentous fungus (*Aspergillus niger* NRC53). One ml of (1×10^8 spores^{-ml}) fungal suspensions was inoculated into 50 ml sterile potato dextrose agar (PDA) medium. 400µl of AgNps colloidal solution was added to each well separately and left for compound diffusion. The plates were incubated for 72 h at 28 ºC and inhibition zones were recorded in millimeters.

3. Results and Discussion

3.1. Gum extract preparation and protein content evaluation

Three different concentrations of *sarcocolla* gum (5,10 and 20 mg/ml) were prepared from the stock aqueous extract of (50 mg/ml, w/v) Fig. 1. Results of protein analysis according to Lowry *et al.* (1951) indicated the presence of higher protein content in stock aqueous extract of yellow-gum (5.458mg/ml), greater than the red-gum (3.161mg/ml) as shown in Table 1.

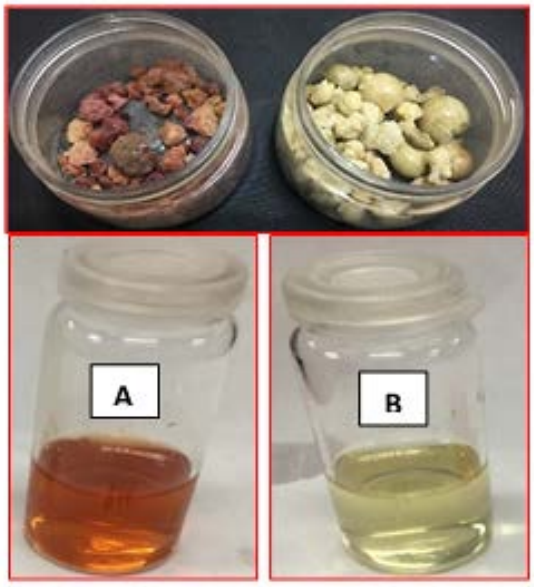

Figure 1. Photograph of *sarcocolla* gum. Stock aqueous extract of red (A) and yellow (B) gum at concentration of 50 mg/ml (w/v).

Table 1. Estimation of protein content of *sarcocolla* red and yellow gum.

Concentration of *sarcocolla* gum (mg/ml) (w/v)		**Protein content (mg/ml)**	
		Red-gum (RG)	**Yellow-gum(YG)**
Stock aqueous extract	50	3.161	5.458
Tested dilutions	5	RG1 (0.316)	YG1 (0.546)
	10	RG2 (0.632)	YG2 (1.092)
	20	RG3 (1.264)	YG3 (2.183)

3.2. Sarcocolla gum-mediated the synthesis of silver nanoparticles

The effect of gum-concentration on the formation of AgNPs was studied. Red and yellow aqueous extracts of 5, 10 and 20 mg/ml (w/v), containing different protein concentrations, were evaluated as reducing and capping agents for biosynthesis of nano-silver. The formation of the AgNPs during the reduction process is indicated first by the formation of reddish to dark brown color after mixing the gum extracts with $AgNO_3$, which can be visually observed. Roy *et al.,* (2015b) emphasized that the colour change resulted from the reduction of silver ions with free electrons excitation, which in turn forms surface plasmon resonance absorption (SPR) bands. In addition, the obtained reddish-brown color of the reaction mixture showed stability without any change at all experiments indicating the stability of the formed AgNPs, in accordance with (Nanda and Majeed, 2014; Ammar *et al.,* 2021).

Results obtained, indicated the ability of *sarcocolla* Gum-proteins to work as reducing and capping agent able to convert $AgNO_3$ into the nano form. All biosynthesized AgNPs were further characterized by UV-spectroscopy, TEM and DLS analyses.

3.3. Characterization of sarcocolla gum AgNPs

3.3.1. UV–Vis spectral analysis

The UV–visible absorption spectra of the AgNPs prepared with different concentrations of red-gum (RG) with 0.316, 0.632 and 1.264 mg/ml protein content respectively are recorded and shown in **Fig. 2.** The UV-vis spectra strong peaks with maxima around 425–440 nm were observed, which correspond to the typical surface plasmon resonance of silver nanoparticles (Kora and Arunachalam, 2012; Mudhafar *et al.*, 2021). In addition, the SPR band broadened with the high gum concentration (RG3) and shifted from 425 to 440 nm, indicating an increase in particle size of AgNPs-RG3, So, the low gum-concentration sample is preferred for synthesis of small sized uniform particles.

Silver-nanoparticles biosynthesized using yellow gum were scanned by UV–Visible spectrophotometer in the ranges of 200 to 800 nm. The result in **Fig. 3** showed that surface plasmon resonance of AgNPs -YG1, YG2 and YG3 appeared at 425, 420 and 420, respectively. The appearance of these peaks is due to the plasmon resonance and inters band transition of AgNPs which proved the biosynthesis of nanoparticles (Ammar *et al.*, 2021). These characteristics are similar to AgNPs synthesized by Kora and Arunachalam, (2012) who detected the formation of AgNPs from Gum tragacanth (*Astragalus gummifer*).

Results obtained in Fig. 3 emphasized that the absorbance intensity increased directly from 2.23 to 2.47 and 3.12 respectively, with increasing the concentration of the yellow-gum extracts. It is also observed that the surface plasmon peak that occurs at 425 nm with the lowest concentration is slowly shifted toward lower wavelength 420nm at high extract concentrations. This shift mainly depends on the particle size and shape (Lee and El-sayed 2006).

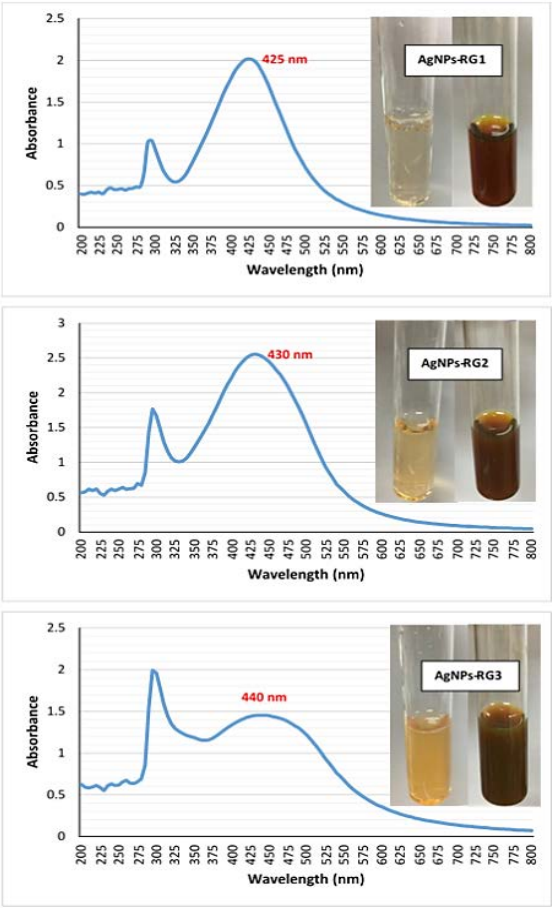

Figure 2. UV–vis spectroscopy of biosynthesized silver-nanoparticle from *Sarcocolla* red gum at 5 (RG1), 10 (RG2) and 20 (RG3) mg/ml concentration.

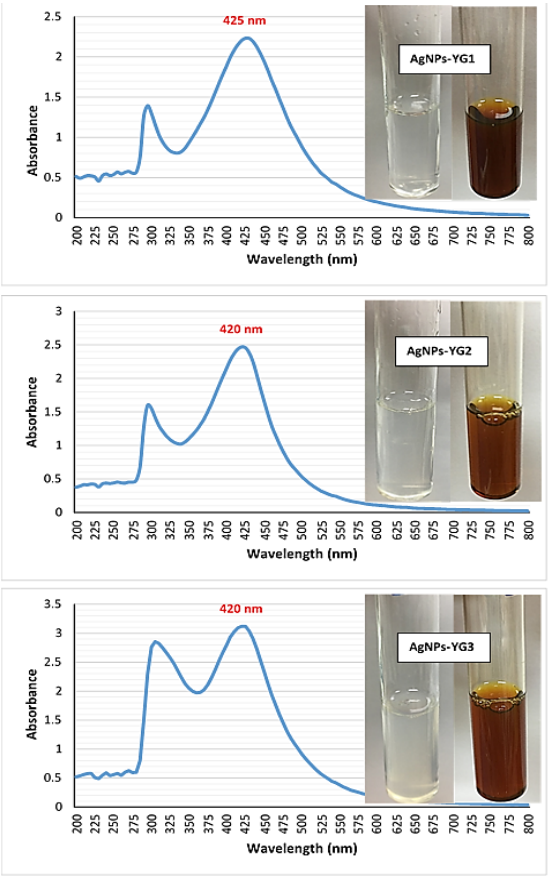

Figure 3. UV–vis spectroscopy of biosynthesized silver-nanoparticle from *Sarcocolla* yellow gum at 5 (YG1), 10 (YG2) and 20 (YG3) mg/ml concentration.

3.3.2. TEM analysis

TEM images of the silver nanoparticles synthesized with 5, 10 and 20 mg/ml red gum showed different shapes varying from spherical, cubic to semi rounded particles with a size range of 9.23±3.66 nm for AgNPs-RG1, 11.36±9.57 nm for AgNPs-RG2 and 15.72±10.79 nm for AgNPs-RG3. TEM analysis (**Fig. 4)** also showed well-dispersed AgNPs biosynthesized using low concentrations of red gum (RG1& RG2). On the other hand, some aggregations were observed with samples prepared with high gum concentration (RG3).

Silver-nanoparticles biosynthesized from yellow gum were spherical to cubic, polydispersed particles with different sizes depending on the gum concentration. AgNPs-YG1 showed sizes from 2.00–17.82 nm, and the average particle size was about 10.92 ± 5.48 nm. When the concentration of yellow gum was increased from 5 to 10 and 20 mg/ml, the particle size of the formed nanoparticles increased to about 12.36 ± 8.37 nm and 15.16 ±6.30 nm respectively as showed in Fig. 5.

The increase in average particle sizes with increase in concentration of the *Astragalus gummifer* gum was also demonstrated by Kora and Arunachalam, (2012). Based on the obtained results, we concluded that the particle size of the nanoparticles can be controlled by varying the gum type and concentration.

The crystallinity of the synthesized nanoparticles was confirmed from the observed clear lattice fringes in high-resolution image, and the concentric rings with intermittent bright dots appeared in the selected-area electron diffraction (SAED) pattern as shown in Figs. 4 and 5.

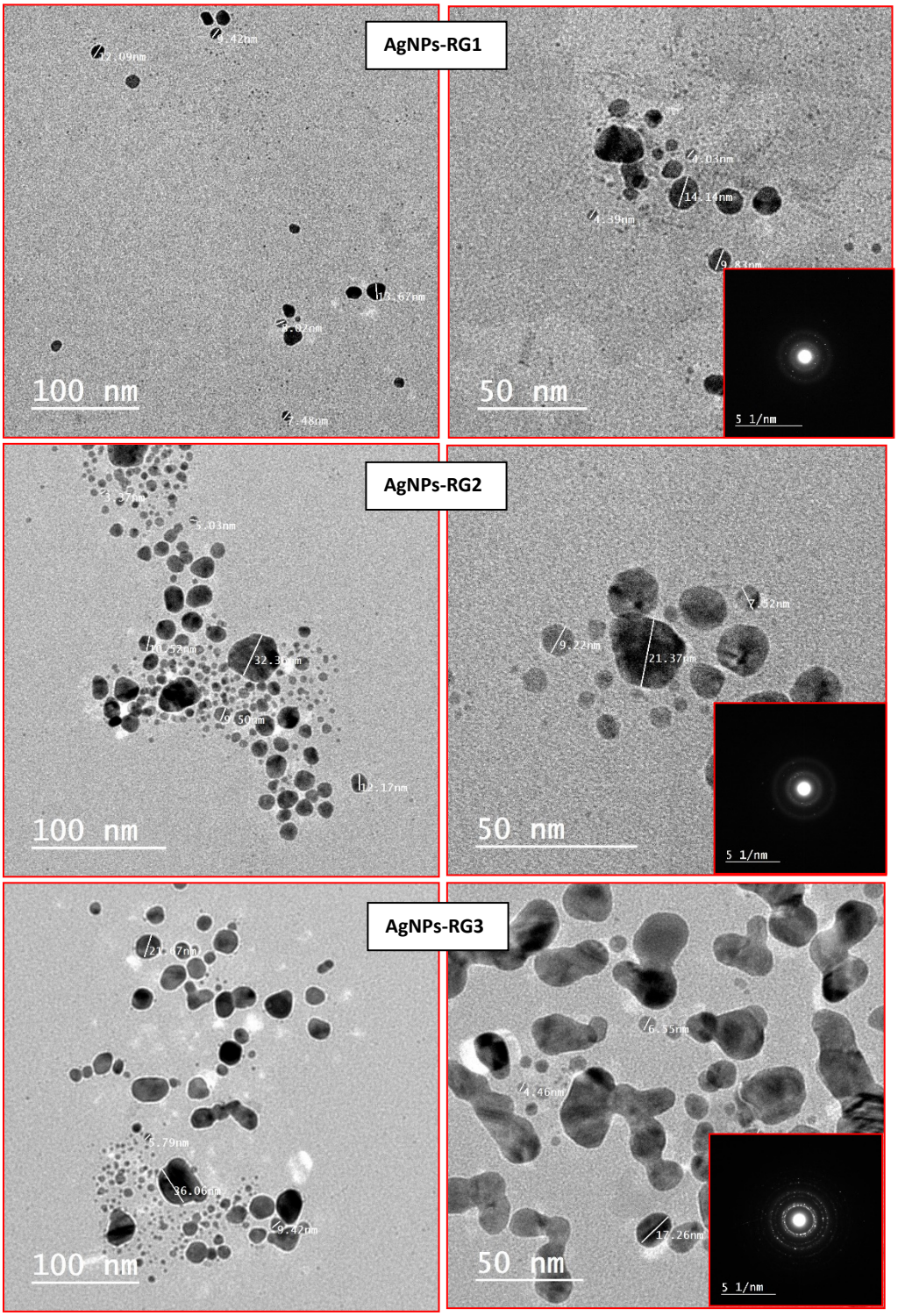

Figure 4. TEM for three synthesized AgNPs using *Sarcocolla* red gum at 5 (RG1), 10 (RG2) and 20 (RG3) mg/ml concentration. Inset shows selected area electron diffraction (SAED) patterns of AgNPs.

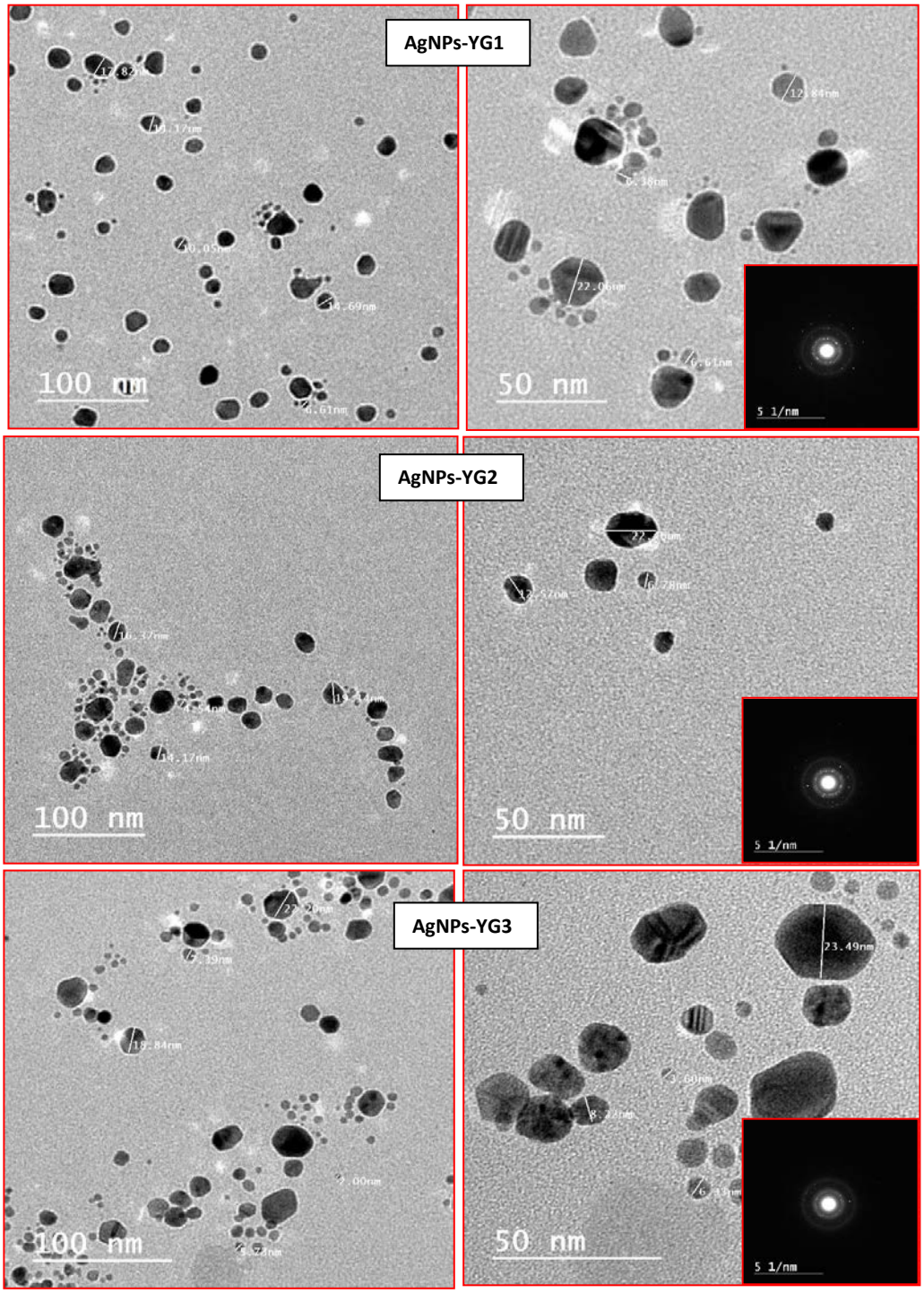

Figure 5. TEM for three synthesized AgNPs using *Sarcocolla* yellow gum at 5 (YG1), 10 (YG2) and 20 (YG3) mg/ml concentration. Inset shows selected area electron diffraction (SAED) patterns of AgNPs.

3.3.3. Dynamic light scatter analysis (DLS)

Dynamic light scatter analysis (DLS) was applied for the most active biosynthesized silver–nanoparticles, AgNPs-RG1 and AgNPs-YG1 to confirm the formation of particles in nano-size. To detect the average size distribution of AgNPs synthesized using low concentrations of red and yellow gums, two different techniques, INTENSITY-Weighted Gaussian Distribution and Zeta potential were applied. Intensity-weight Gaussian Distribution was found to be 48.2 and 74.2 nm, respectively. And their Zeta potential were -41.32 and −30.54 mv, respectively, which indicated their good stability Fig. 6.

High negative values of AgNPs-RG1 and YG1 appeared clearly to be advantageous for long-term colloidal stability, as mentioned by Eltarahony *et al.* (2018), who indicated that the values less than (−25 mV) or greater than (+25 mV) display higher electrical charge on nano-particles surface, which prevents agglomeration, but Alshammari and Abd El Aty (2022), showed slightly low surface charges of -6.70, -8.73 and 0.16 mv

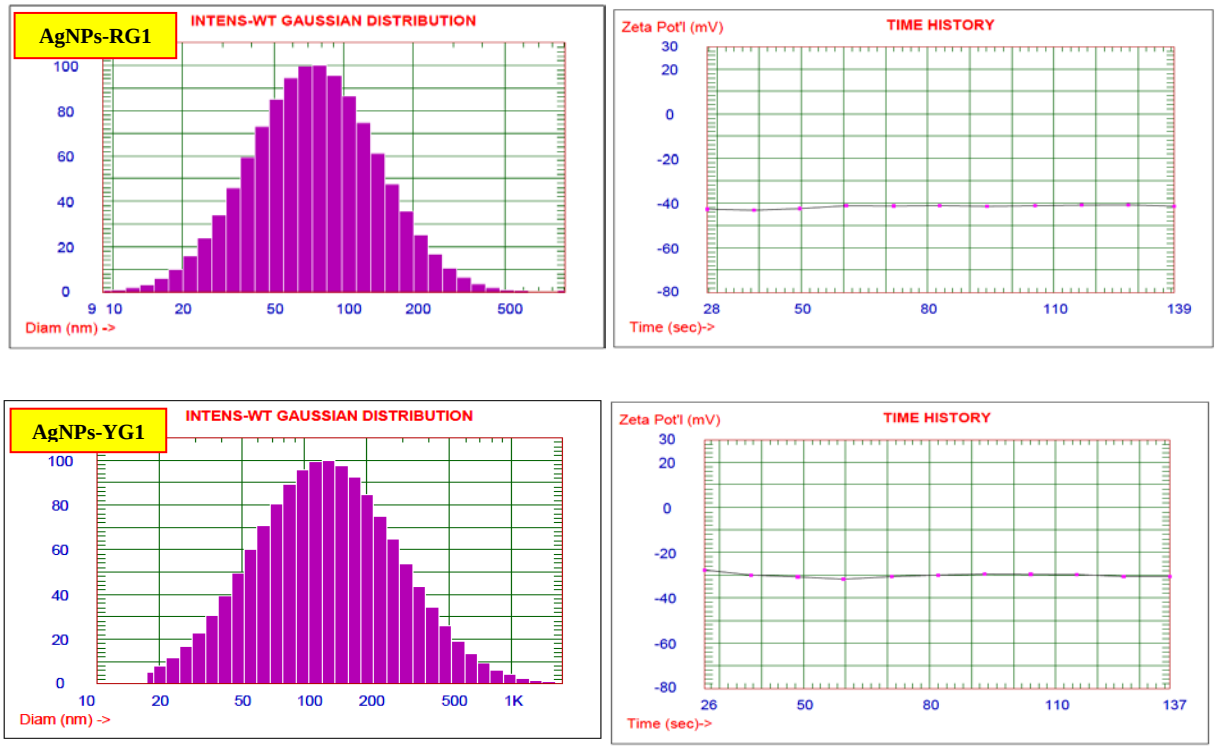

Figure 6. Gaussian distribution and Zeta potential of AgNPs biosynthesized by RG1 and YG1.

3.4. Biomedical applications of sarcocolla gum-AgNPs

3.4.1. Cytotoxicity assay

Silver-nanoparticles biosynthesized from aqueous extract of red gum (RG1, RG2, RG3) and that prepared using aqueous extract of yellow gum (YG1, YG2, YG3) were tested for their cytotoxic effect against five human cancer cells and one normal cells Table 2. The results, expressed as IC_{50} values are reported in Table 3.

The results showed that, out of three biosynthesized silver–nanoparticles of red gum aqueous extract, the AgNPs-RG1 was the most active and possessed high cytotoxic effect against four cancer cells, namely A549, pc3, Mcf7 and paca2 with IC_{50} values (88.4,75.6, 72.2& 55.0 ug/ml, respectively) and showed low cytotoxic effect (20 % at 100ug/ml) against human normal cells (BJ-1). On the other hand, AgNPs-RG2 showed cytotoxic effect against only paca2 cell line with IC 50 (47.0ug/ml) and AgNPs-RG3 showed only cytotoxic effect against mcf-7 with IC_{50} (74.4ug/ml), but two nanoparticles of (AgNPs-RG2 and AgNPs-RG3) showed highly cytotoxic effect against normal cells IC_{50} (46.8 and 76.4ug/ml). Devanesan *et al.*, (2020) showed good cytotoxicity of As-AgNPs biosynthesized from the plant *Ferula foetida* (asafoetida gum) against MCF-7 cell lines. Good cytotoxicity of silver-nanoparticles against human cancerous cells mainly occurs due to the high proliferation rate and abnormal metabolism of cancerous cells, which in turn causes the high uptake of nanoparticles by these cells more than normal cells (Park *et al.*, 2010; Madunić *et al.*, 2018).

Results also emphasized that silver-nanoparticles biosynthesized from different concentrations of yellow gum aqueous extract possessed various cytotoxic activity. AgNPs-YG1 showed high cytotoxic effect against three cancer cells (PC3, MCF-7 and paca2) with IC_{50} values (75.0, 82.8 and 81,6ug/ml respectively), and normal cells (BJ-1) with IC_{50} value (81.8ug/ml). Another study of Sánchez-Navarro *et al.*, (2018) also confirmed that the lower concentration of *Annona muricata* aqueous extract exhibited cytotoxicity oral fibroblasts. On the other hand, AgNPs-YG3 has high cytotoxic effect against tow cancer cells (MCF-7 and paca2) with IC_{50} values (52.6 and 90.3ug/ml respectively), with low cytotoxic effect against normal cells (Bj-1) 13.6% at 100 ug/ml. AgNPs-YG2 possessed high cytotoxic effect against only breast cancer cell (IC50=72.2).

The cytotoxic effect of the AgNPs-RG1 and AgNPs-YG1 indicates the possible application of these AgNPs as chemotherapeutic agents (Ahamed and AlSalhi, 2010).

Table 2. Cytotoxic effect of *Sarcocolla* Gum-AgNPs against five different human cancer cell lines and normal cell line (BJ-1).

Treatment	Cytotoxicity %*					
	A549	PC3	HCT-116	MCF-7	Paca2	Normal cells (BJ-1)
AgNPs-RG1	55.3	60.8	18.6	64.6	91.5	20.8
AgNPs-RG2	14.5	46.4	4.4	27	97	100
AgNPs-RG3	19.9	10	9.1	65	55.7	69.5
AgNPs-YG1	22.5	58.3	27.7	57.9	94.3	64.6
AgNPs-YG2	22.2	2.8	21.7	64	40.3	38.2
AgNPs-YG3	36.2	26.6	28.4	76	52.1	13.6
Doxorubicin	98.2	96.6	99.4	97.6	98.3	99.8

* Cytotoxicity % of AgNPs measured at 100ug/ml against different cancer cell lines.

Table 3. IC $_{50}$ µg/ml of *Sarcocolla* Gum-AgNPs samples.

Treatment	IC50 ug/ml					
	A549	PC3	HCT-116	MCF-7	Paca2	BJ-1
AgNPs-RG1	88.4	75.6	-	72.2	55.0	-
AgNPs-RG2	-	-	-	-	47.0	46.8
AgNPs-RG3	-	-	-	74.4	81.6	76.4
AgNPs-YG1	-	75.0	-	82.8	50.7	81,8
AgNPs-YG2	-	-	-	72.2	-	-
AgNPs-YG3	-	-	-	52.6	90.3	-
Doxorubicin	21.6	21.6	26.1	37.6	28.3	13.5

3.4.2. Cellular morphology

The effects of the *Sarcocolla*-AgNPs-RG1 and AgNPs-YG1 on cellular morphology were observed directly using Inverted microscope as shown in Fig. 7. Untreated cancer cells were homogeneously distributed on a cultured field, exhibiting a uniform polygonal shape. Following incubation with the silver-nanoparticles, various morphological changes were observed. Photos also showed that exposure of the cells to the AgNPs transformed the shapes of the cells from polygonal to circular and resulted in cell shrinkage. The non-active nanopartcles did not show any significant morphological change. Notably, these morphological alterations were observed at 100 µg/ml concentration.

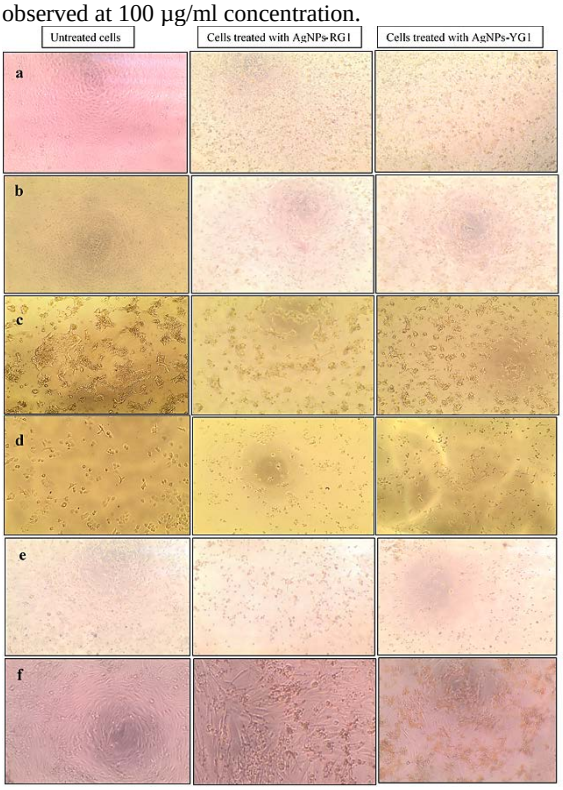

Figure 7. Microscopic examination of *Sarcocolla*-AgNPs-RG1 and AgNPs-YG1 treated and untreated cells of (a) A549, (b) PC3, (c) HCT-116, (d) MCF-7, (e) Paca2, (f) Normal cells (BJ-1).

3.4.3. Antimicrobial assay

Antibacterial and antifungal activities of the synthesized red and yellow gum-mediated AgNPs with different sizes and shapes were investigated against Gram-positive (*S. aureus*, *B. subtilis*, *L. cereus*) and Gram-negative (*E. coli*, *S. enterica*) bacteria using the agar diffusion method. Results in Table 4 indicated that AgNPs-RG1, RG2 and YG1 exhibited broad spectrum antimicrobial effects against all tested pathogenic bacteria, yeast and fungi, but no antimicrobial activity was displayed by AgNPs-RG3, YG2 and YG3, this negative effect may be due to large sized particles and aggregations.

Figs. 8 and 9 showed good antibacterial activity of AgNPs-RG1, RG2 and AgNPs-YG1 against gram-positive strains with inhibition zone diameter in range from 19-25 mm and from 19-26 mm respectively. Also, the gram-negative strains were highly inhibited after treatment with AgNPs-YG1 (IZD in range from 22-24 mm), followed by AgNPs-RG1 (IZD in range from 19-23 mm) and AgNPs-RG2 (IZD in range from 19-22 mm).

Ramdath *et al.* (2021) emphasized that the bactericidal effects observed in all bacterial strains caused as a result of releasing silver-cations. Researchers showed the ability of AgNPs to bind on to the surface of bacterial cells and directly affect the sulphur and phosphorous moieties of the cell-membrane; therefore, the cell metabolism has been failed leading to the bacterial death (Rawani *et al.*, 2013; Bindhu and Umadevi, 2015).

Results also observed that both the AgNPs-RG1 and YG1 solutions exhibit similar antifungal activity in the unicellular yeast *C. albicans* (21 and 20 mm respectively) and the filamentous fungus *A. niger* (17 and 18 mm respectively), but AgNPs -RG2 showed only an inhibitory effect against *C. albicans* 22mm.

In most cases, the antifungal mechanism of silver ions on microorganisms, due to their effects on the function of membrane-bound enzymes, inactivation of cellular proteins and enzymes essential to DNA replication (Min et al., 2009; Ammar et al., 2021).

In general, the findings suggested the AgNPs-RG1 and YG1 as good potential antibacterial and antifungal agents.

Table 4. Antibacterial and antifungal activity of the biosynthesized AgNps against pathogenic bacteria and fungi.

Samples (400µl/ well)	Inhibition zone diameter (IZD)						
	Gram-negative bacteria		**Gram-positive bacteria**			**Yeast**	**Fungi**
	Escherichia coli ATCC25922	*Salmonella enterica* ATCC25566	*Staphylococcus aureus* ATCC29213	*Bacillus subtilis* ATCC6633	*Lactobacillus cereus* ATCC14579	*Candida albicans* ATCC10321	*Aspergillus niger* NRC53
Red -Gum extract (C)	N.A	N.A	N.A	N.A	N.A	N.A	N.A
AgNPs RG1	23±0.17	19±0.28	25±0.42	22±0.16	21±0.35	21±0.18	17±0.17
AgNPs RG2	22±0.38	19±0.44	19±0.17	22±0.51	25±0.24	22±0.34	N.A
AgNPs RG3	N.A	N.A	N.A	N.A	N.A	N.A	N.A
Yellow- Gum extract (C)	N.A	N.A	N.A	N.A	N.A	N.A	N.A
AgNPs YG1	24±0.18	22±0.17	26±0.44	19±0.31	21±0.17	20±0.25	18±0.28
AgNPs YG2	N.A	N.A	N.A	N.A	N.A	N.A	N.A
AgNPs YG3	N.A	N.A	N.A	N.A	N.A	N.A	N.A

N.A. no activity

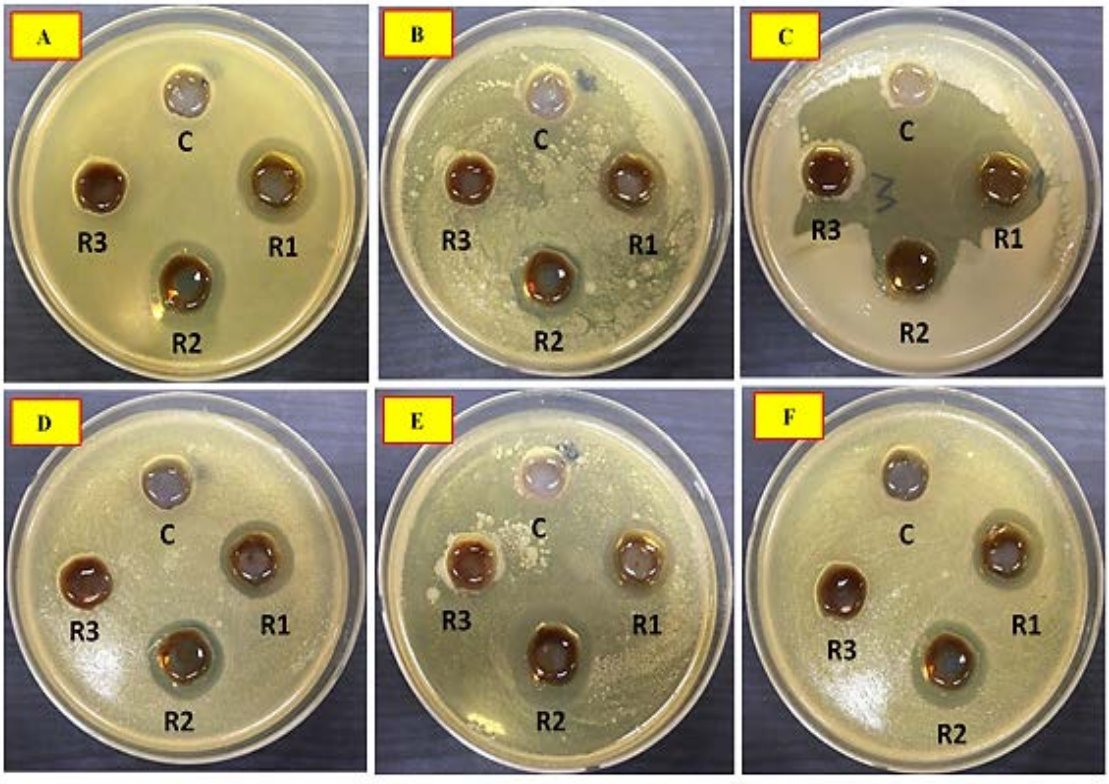

Figure 8. Photos of the antimicrobial effect of biosynthesized AgNPs using *sarcocolla* red gum at 5 (RG1), 10 (RG2) and 20 (RG3) mg/ml concentration against *E. coli* (A), *S. enterica* (B), *S. aureus* (C), *B. subtilis*(D). *L. cereus* (E) and *C. albicans* (F).

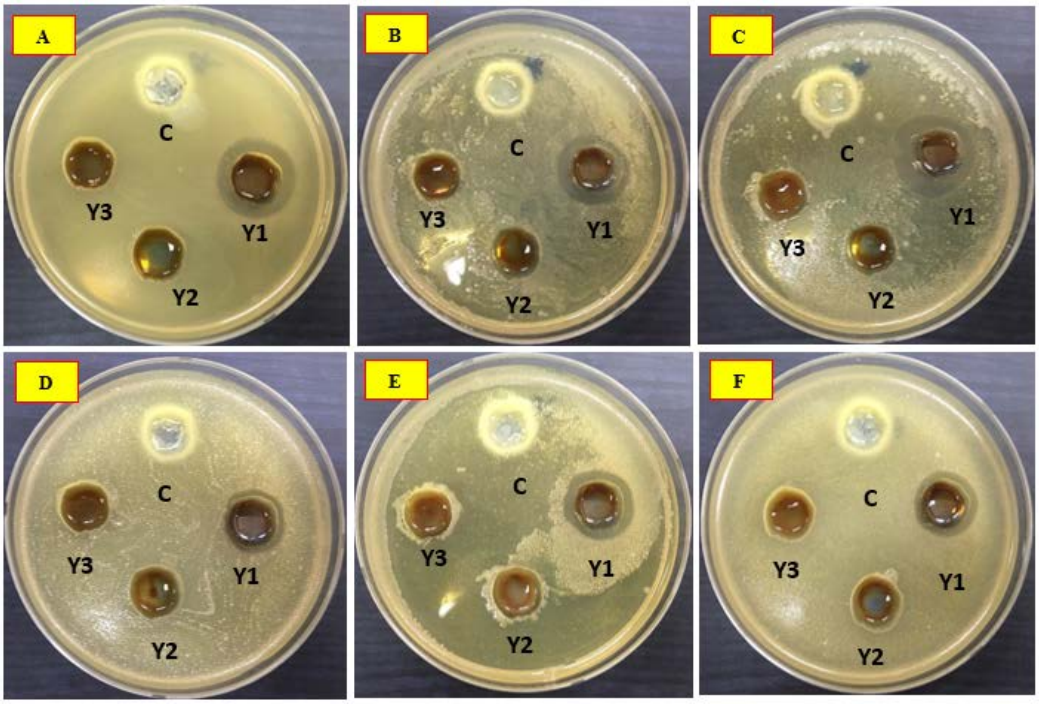

Figure 9. Photos of the antimicrobial effect of biosynthesized AgNPs using *sarcocolla* yellow gum at 5 (YG1), 10 (YG2) and 20 (YG3) mg/ml concentration against *E. coli* (A), *S. enterica* (B), *S. aureus* (C), *B. subtilis*(D). *L. cereus* (E) and *C. albicans* (F).

4. Conclusion

This paper, showed a novel simple, cost effective, eco-friendly green method using aqueous extract of red and yellow *Astragalus sarcocolla* gum. All characterization studies emphasized the biosynthesis of stable nanoparticles with different shapes and sizes specially at low gum concentrations, which in turn indicated the good application of *sarcocolla* gum as a reducing and stabilizing agent instead of using toxic chemical entities. Anticancer and antimicrobial potential of six gum-mediated silver nanoparticles was investigated. AgNPs-RG1 and AgNPs-YG1 showed the best cytotoxic effects against four cancer cells namely A549, pc3, Mcf7 and paca2, and the inverted microscope examination showed various morphological changes in the cells treated with AgNPs compared with untreated cancer cells, which confirmed the toxic effect of AgNPs. In addition, AgNPs-RG1, RG2 and AgNPs-YG1 exhibited good inhibition zones against all tested pathogenic bacteria, yeast and fungi.

Acknowledgement

The authors extend their appreciation to the Deanship of Scientific Research, University of Hafr Al Batin, for funding this work through the research group project No (0006-1443-S).

Conflict of interest

The authors declare that they have no conflict of interests.

References

Ababutain I M. 2017. Antimicrobial Activity and Phytochemical Screening of Sarcocolla Gum Resin. *Pak. J. Biol. Sci.* **20 (11)**: 571-576. DOI: 10.3923/pjbs.2017.571.576

Abd El Aty A A and Ammar H A. 2016. Potential characterization and antimicrobial applications of newly bio-synthesized silver and copper nanoparticles using the novel marine-derived fungus Alternaria tenuissima KM651985. *Res. J. Biotechnol.* **11(8):** 71-82.

Abd El Aty A A and Zohair M M. 2020. Green-synthesis and optimization of an eco-friendly nanobiofungicide from Bacillus amyloliquefaciens MH046937 with antimicrobial potential against phytopathogens. *Environ. Nanotechnol. Monit. Manag.*,**14**,100309.https://doi.org/10.1016/j.enmm.2020.100309

Abd El Aty A A, Mohamed A A, Zohair M M and Soliman A A F. 2020. Statistically controlled biogenesis of silver nano-size by Penicillium chrysogenum MF318506 for biomedical application. *Biocatal. Agric. Biotechnol*, **25**: 101592. https://doi.org/10.1016/j.bcab.2020.101592

Ahamed M and AlSalhi M S. 2010. Siddiqui MKJ. Silver nanoparticle applications and human health. *Clin Chim Acta*. **411**: 1841–1848. doi:10.1016/j.cca.2010.08.016

Akram M, Iqbal M, Daniyal M and Khan A U. 2017. "Awareness and current knowledge of breast cancer," *Biol. Res.*, **50 (1):**1–23.

Alharbi RM, Soliman A A F and Abd El Aty A A. 2020. COMPARATIVE STUDY ON BIOSYNTHESIS OF VALUABLE ANTIMICROBIAL AND ANTITUMOR NANO-SILVER USING FRESH WATER GREEN AND BLUE-GREEN MICROALGAE. *J. Microbiol. Biotechnol. Food Sci.*, **10(2)** https://www.jmbfs.org/wp-content/uploads/2020/10/1852-Main-document-manuscript-preprint.pdf

Alharbi R M, Alshammari S O and Abd El-Aty A A. Statically-improved Fungal Laccase-mediated the Biogenesis of Silver Nanoparticles with Antimicrobial Applications. *J. Appl. Pharm. Sci..,* **13(01),** 241-253, 2023. DOI: 10.7324/JAPS.2023.130105

Alshammari S O and Abd El Aty A A. 2022. Statically controlled mycogenic-synthesis of novel biologically active silver-nanoparticles using Hafr Al-Batin desert truffles and its antimicrobial efficacy against pathogens. *Saudi J Biol Sci.,* **29:** 103334. https://doi.org/10.1016/j.sjbs.2022.103334.

Ammar H A, Abd El Aty A A and El Awdan S A. 2021. Extracellular myco-synthesis of nano-silver using the fermentable yeasts Pichia kudriavzeviiHA-NY2 and Saccharomyces uvarumHA-NY3, and their effective biomedical applications. *Bioprocess Biosyst Eng*., **44 (4):** 841-854. https://doi.org/10.1007/s00449-020-02494-3

Bindhu M R and Umadevi M. 2015. "Antibacterial and catalytic activities of green synthesized silver nanoparticles," Spectrochimica Acta Part A: *Mol. Biomol. Spectrosc.,* **135**:373–378.

Bisht S, Mizuma M, Feldmann G. et al., 2010. "Systemic administration of polymeric nanoparticle-encapsulated curcumin (NanoCurc) blocks tumor growth and metastases in preclinical models of pancreatic cancer," *Mol. Cancer Ther.,* **9 (8):** 2255–2264.

Daniel M and Astruc D. 2004. Gold nanoparticles: assembly, supramolecular chemistry, quantum-size-related properties, and applications toward biology, catalysis, and nanotechnology. *Chem Rev*. **104**: 293–346.

Demchenko V, Riabov S, Sinelnikov S, Radchenko O, Kobylinskyi S and Rybalchenko N. 2020. "Novel approach to synthesis of silver nanoparticles in interpolyelectrolyte complexes based on pectin, chitosan, starch and their derivatives," *Carbohydr. Polym..*, **242**, Article ID 116431.

Devanesan S, Ponmurugan K, AlSalhi MS and Al-Dhab NA. 2020. Cytotoxic and Antimicrobial Efficacy of Silver Nanoparticles Synthesized Using a Traditional Phytoproduct, Asafoetida Gum. *Int. J. Nanomedicine*. **15**: 4351–4362.

Eltarahony M, Zaki S and Abd-El-Haleem D. 2018. Concurrent Synthesis of Zero- and One-Dimensional, Spherical, Rod-, Needle-, and Wire-Shaped CuO Nanoparticles by Proteus mirabilis 10B, *J. Nanomater.,* 1849616: https://doi.org/10.1155/2018/1849616

Kokila T, Ramesh P S and Geetha D. 2015. Biosynthesis of silver nanoparticles from Cavendish banana peel extract and its antibacterial and free radical scavenging assay: a novel biological approach. *Appl Nanosci.* **5**: 911–20. doi:10.1007/s13204-015-0401-2

Kora A J and Arunachalam J. 2012. Green fabrication of silver nanoparticles by gum tragacanth (Astragalus gummifer): a dual functional reductant and stabilizer. *J Nanomater*. **1–8**. doi:10.1155/2012/869765.

Kora A J, Beedu S R and Jayaraman A. 2012. Size-controlled green synthesis of silver nanoparticles mediated by gum ghatti (*Anogeissus latifolia*) and its biological activity. *Organic Med Chem Lett.* **2**: 17. doi:10.1186/2191-2858-2-17.

Lee , Kyeong-Seok and El-Sayed M A. 2006. Gold and silver nanoparticles in sensing and imaging: sensitivity of plasmon response to size, shape, and metal composition. *J Phys Chem B.* **110 (39):** 19220-5. doi: 10.1021/jp062536y.

Lee S and Jun B-H. 2019. "Silver nanoparticles: synthesis and application for nanomedicine," *Int J Mol Sci* , **20 (4):** 865.

Li T, Park H G and Choi S-H. 2007. γ-Irradiation-induced preparation of Ag and Au nanoparticles and their characterizations. *Mater Chem Phys.* **105**: 325–30. doi:10.1016/j.matchemphys.2007.04.069.

Lowry O H, Rosebrough NJ, farr AL and Randall RJ. 1951. Protein measurement with the folin Phenol reagent, *J. Biol. Chem*., **193**: 265-275.

Mackey T K, Liang B A, Cuomo R, Hafen R, Brouwer K C and Lee D E. 2014. "Emerging and reemerging neglected tropical diseases: a review of key characteristics, risk factors, and the policy and innovation environment," *Clin. Microbiol. Rev.* **27 (4):** 949–979.

Madunić J, Madunić IV, Gajski G, Popić J and Garaj-Vrhovac V, 2018. Apigenin: a dietary flavonoid with diverse anticancer properties. *Cancer Lett.* **413**: 11–22. doi:10.1016/j.canlet.2017.10.041

Mehndiratta P and Jain A. 2013. Srivastava S, Gupta N. Environmental pollution and nanotechnology. *Environ Pollut.* **2**: 49–58. doi:10.5539/ep.v2n2p49.

Min JS, Kim KS, Kim SW, Jung JH, Lamsal K, Kim SB, Jung M and Lee YS. 2009. Effects of colloidal silver nanoparticles on sclerotium-forming phytopathogenic fungi. *Plant Pathol J.* **25:** 376–380.

Mosmann T. 1983. Rapid colorimetric assay for cellular growth and survival: application to proliferation and cytotoxicity assays. *J. Immunol. Methods* **65**: 55–63.

Mudhafar M, Zainol I, Alsailawi H A and Aiza Jaafar C N. 2021. Green Synthesis of Silver Nanoparticles using Neem and Collagen of Fish Scales as a Reducing and Stabilizer Agents. *Jordan J. Biol. Sci.* **14**: 899 – 903. https://doi.org/10.54319/jjbs/140503

Murali Krishna I, Bhagavanth Reddy G, Veerabhadram G and Madhusudhan A. 2015. Ecofriendly green synthesis of silver nanoparticles using salmalia malabarica: synthesis, characterization, antimicrobial, and catalytic activity studies. *Appl Nanosci*. doi:10.1007/s13204-015-0479-6.

Nanda A and Majeed S. 2014. Improved bactericidal property of silver nanoparticles from *Penicillium pinophilum* (MTCC 2192) in a combined form with carbicillin and moxifoxacin. *Int J Pharm Pharm Sci.* **6**:609–612.

Pandey S and Mishra SB. 2014. Catalytic reduction of p-nitrophenol by using platinum nanoparticles stabilized by guar gum. *Corbopol.* **113**: 525–31. doi:10.1016/j.carbpol.2014.07.047.

Pandey S, Mishra SB. 2016. Au nanocomposite based chemiresistive ammonia sensor for health monitoring. *Am Chem Soc*. **1(1):** 55–62. doi:10.1021/ acssensors.5b00013.

Park EJ, Yi J, Kim Y, Choi K and Park K. 2010. Silver nanoparticles induce cytotoxicity by a Trojan-horse type mechanism. Toxicol in Vitro. **24**: 872–878. doi:10.1016/j.tiv.2009.12.001

Parveen M, Ahmad F, Malla AM and Azaz S. 2016. Microwave-assisted green synthesis of silver nanoparticles from Fraxinus excelsior leaf extract and its antioxidant assay. *Appl Nanosci*. **6**: 267–76. doi:10.1007/s13204-015-0433-7

Qi F, Zhao L, Zhou A et al. 2015. "+e advantages of using traditional Chinese medicine as an adjunctive therapy in the whole course of cancer treatment instead of only terminal stage of cancer," *Biosci. Trends.* **9 (1):** 16–34.

Raghavendra G M, Jung J, kim D and Seo J. 2016. "Step-reduced synthesis of starch-silver nanoparticles," *Int. J. Biol. Macromol.* **I 86**:126–128.

Raju D, Paneliya N and Mehta U J. 2014. Extracellular synthesis of silver nanoparticles using living peanut seedling. *Appl. Nanosci.* **4**: 875–9. doi:10.1007/s13204-013-0269-y

Ramdath S, Mellem J and Mbatha LS. 2021. Anticancer and Antimicrobial Activity Evaluation of Cowpea-Porous-Starch-Formulated Silver Nanoparticles. *J. Nanotechnol.*. Article ID 5525690, 13 pages. https://doi.org/10.1155/2021/5525690

Rastogi L, Sashidhar RB, Karunasagar D and Arunachalam J. 2014. Gum kondagogu reduced/stabilized silver nanoparticles as direct colorimetric sensor for the sensitive detection of Hg2+ in aqueous system. Talanta. **118**: 111–7. doi:10.1016/j.talanta.2013.10.012.

Rawani A, Ghosh A and Chandra G. 2013. "Mosquito larvicidal and antimicrobial activity of synthesized nano-crystalline silver particles using leaves and green berry extract of Solanum nigrum L. (Solanaceae: Solanales)," *Acta Trop.* **128 (3):** 613–622.

Roy K, Sarkar C K and Ghosh C K. 2015a. Photocatalytic activity of biogenic silver nanoparticles synthesized using yeast (*Saccharomyces cerevisiae*) extract. *Appl Nanosci*. **5(8):** 953–959 35.

Roy K, Sarkar CK and Ghosh CK. 2015b. Plant-mediated synthesis of silver nanoparticles using parsley (*Petroselinum crispum*) leaf extract: spectral analysis of the particles and antibacterial study. *Appl Nanosci*. **5**: 945–51. doi:10.1007/s13204-014-0393-3

Sánchez-Navarro M C, Ruiz-Torres CA, Niño-Martínez N, et al. 2018. Cytotoxic and bactericidal effect of silver nanoparticles obtained by green synthesis method using annona muricata aqueous extract and functionalized with 5-fluorouracil. *Bioinorg Chem Appl*. 1–8. doi:10.1155/2018/6506381.

Song JY and Kim BS. 2009. Rapid biological synthesis of silver nanoparticles using plant leaf extracts. *Bioprocess Biosyst Eng.* **32**: 79–84. doi:10.1007/s00449-008-0224-6

Vasan N, Baselga J and Hyman D M. 2019. "A view on drug resistance in cancer," *Nature*. **575 (7782):** 299–309.

Wang X, Yuan L, Deng H and Zhang Z. 2021. "Structural characterization and stability study of green synthesized starch stabilized silver nanoparticles loaded with Isoorientin," *Food Chem*, **338**, Article ID 127807.